INTEGRATION OF INTENSITY EDGE INFORMATION INTO THE REACTION-DIFFUSION STEREO ALGORITHM

Atsushi Nomura
Faculty of Education, Yamaguchi University, Yoshida 1677-1, Yamaguchi, Japan

Makoto Ichikawa
Faculty of Letters, Chiba University, Yayoi-cho 1-33, Inage-ku, Chiba, Japan

Koichi Okada
Education Promoting Center, Yamaguchi University, Yoshida 1677-1, Yamaguchi, Japan

Hidetoshi Miike
Graduate School of Science and Engineering, Yamaguchi University, Tokiwadai 2-16-1, Ube, Japan

Keywords: Stereo algorithm, Reaction-diffusion equation, Anisotropic diffusion, PDE approach, Visual integration.

Abstract: The present paper proposes a visual integration algorithm that integrates intensity edge information into a stereo algorithm. The stereo algorithm assumes two constraints of continuity and uniqueness on disparity distribution. Since depth discontinuity around object boundaries does not satisfy the continuity constraint, it causes numerous errors in stereo disparity detection. In order to reduce the errors due to the depth discontinuity, we propose a new algorithm that integrates intensity edge information into the stereo algorithm. The stereo algorithm utilizes reaction-diffusion equations, in which diffusion coefficients control the continuity constraint. Thus, we introduce anisotropic diffusion fields into the reaction-diffusion equations; that is, we modulate the diffusion coefficients according to results of edge detection applied to image intensity distribution. We demonstrate how the proposed algorithm works around areas having depth discontinuity and confirm quantitative performance of the algorithm in comparison to other stereo algorithms.

1 INTRODUCTION

The cooperative stereo algorithm proposed by Marr and Poggio (Marr and Poggio, 1979) assumes two constraints: uniqueness and continuity on stereo disparity distribution. The uniqueness constraint states that a particular point in a stereo disparity distribution has only one stereo disparity level except for transparent object; the continuity constraint states that stereo disparity varies continuously over object surfaces. Although most areas in stereo disparity distribution satisfy the continuity constraint, areas having depth discontinuity such as object boundaries do not satisfy the continuity constraint. Thus, stereo algorithms assuming the continuity constraint tend to provide numerous errors in areas having the depth discontinuity.

The problem due to discontinuity is one of the central issues in image processing and computer vision research. We usually apply the Gaussian filter to distribution of visual properties such as intensity, disparity or motion around spatial neighboring points, in order to smooth the distribution. We can utilize a diffusion equation instead of the Gaussian filter. However, since a smoothing process or a diffusion process across the discontinuity causes unexpected smoothing or diffusion on the visual properties, there are also numerous errors around areas having the discontinuity. In order to solve the problem due to the discontinuity, several algorithms introduced anisotropy into the Gaussian filter or the diffusion process. An edge detection algorithm proposed by Perona and Malik is

Nomura A., Ichikawa M., Okada K. and Miike H. (2009).
INTEGRATION OF INTENSITY EDGE INFORMATION INTO THE REACTION-DIFFUSION STEREO ALGORITHM.
In *Proceedings of the Fourth International Conference on Computer Vision Theory and Applications*, pages 580-586
DOI: 10.5220/0001821005800586

one of the most famous algorithms having anisotropic diffusion (Perona and Malik, 1990).

When focusing on stereo disparity detection, we can find many state-of-the-art stereo algorithms (Scharstein and Szeliski, 2002), some of which handle the problem due to depth discontinuity or its related occluding boundary problem. The cooperative algorithm (Marr and Poggio, 1979) mentioned above is one of the most widely known and primitive algorithms. Zitnick and Kanade proposed a modern cooperative algorithm (Zitnick and Kanade, 2000), which assumes the two constraints and also simultaneously provides a solution to solve the occluding boundary problem. The belief-propagation algorithm (Klaus et al., 2006) and the graph-cuts algorithm (Deng et al., 2007) are also attracting much attention from computer vision researchers, since they achieved good performance on stereo disparity detection. Some of the algorithms can also detect occlusion areas and thus can partially avoid the problem due to the depth discontinuity.

Several researchers have proposed to utilize reaction-diffusion systems or equations in image processing and computer vision research. Kuhnert et al. found that a reaction-diffusion system described with reaction-diffusion equations works as an optical memory device and visualizes edges and segments of patterns from image intensity distribution (Kuhnert, 1986; Kuhnert et al., 1989). Adamatzky et al. proposed novel computer architecture that performs image processing with a reaction-diffusion system (Adamatzky et al., 2005); they also proposed computer algorithms utilizing the reaction-diffusion equations and named a class of the algorithms 'reaction-diffusion algorithm'. Suzuki et al. realized a reaction-diffusion system with large-scale integrated circuits for an application to finger-print identification (Suzuki et al., 2005). Ueyama et al. proposed a model described with a reaction-diffusion equation for explaining figure-ground separation observed in the human motion perception (Ueyama et al., 1998). The authors applied the reaction-diffusion equations to edge detection and segmentation in image processing (Nomura et al., 2003).

The previous stereo algorithm proposed by the authors also utilizes the reaction-diffusion equations (Nomura et al., 2009). The algorithm consists of multi-sets of the reaction-diffusion equations; each set governs areas of its corresponding disparity level, in accordance with the cooperative algorithm. Diffusion processes in the reaction-diffusion equations realize the continuity constraint; a mutual inhibition mechanism built in the multi-sets realizes the uniqueness constraint. However, the algorithm did not achieve satisfactory performance on disparity detection, in particular, in areas having depth discontinuity.

Reaction-diffusion equations were originally proposed as mathematical models for explaining pattern formation or signal propagation observed in natural systems such as chemical and biological systems. The equations couple diffusion equations with reaction terms describing chemical reaction or biological phenomena; they are composed of time-evolving partial-differential equations. For example, the FitzHugh-Nagumo type reaction-diffusion equations are a simplified model of equations describing signal propagation along a nerve axon (FitzHugh, 1961; Nagumo et al., 1962). By modeling visual functions and realizing their computational algorithms with the reaction-diffusion equations, we are trying to support the algorithms in their biological background, even if we do not have direct evidence that connects each of the algorithms with the human visual perception. The authors believe that such the biologically motivated algorithms are interesting from both scientific and engineering points of view.

In this position paper, we focus on the problem due to depth discontinuity and propose an idea of a visual integration algorithm that integrates intensity edge information into the reaction-diffusion stereo algorithm. Previous psycho-physical studies provided several evidences showing that the human vision system reconstructs depth distribution from combination of several kinds of visual information such as binocular stereopsis, motion, texture and shading (Landy et al., 1995). We believe that integration of edge information into the stereo algorithm brings better performance, also in the case of stereo disparity detection. Since the reaction-diffusion stereo algorithm realizes the continuity constraint with diffusion processes, weak diffusion prevents the stereo disparity information from diffusing. Thus, in order to realize the algorithm of the integration, we introduce anisotropic diffusion fields (Perona and Malik, 1990; Black et al., 1998) into the reaction-diffusion equations; we can expect that anisotropic diffusion fields modulated by depth edge information prevent disparity information from diffusing across depth edges. However, it is difficult to detect areas having depth discontinuity prior to stereo disparity detection. Thus, we utilize areas having intensity edges instead of areas having the depth discontinuity; another reaction-diffusion algorithm designed for edge detection provides the intensity edge information (Nomura et al., 2008). We realize the full reaction-diffusion system that detects stereo disparity and intensity edges; we provide results of the intensity edge detection to anisotropic dif-

fusion fields in the proposed stereo algorithm. We confirm how the proposed algorithm works around the areas having depth discontinuity for test stereo image pairs provided on the Middlebury website (http://vision.middlebury.edu/stereo/) (Scharstein and Szeliski, 2002). In addition, we evaluate the quantitative performance of the stereo algorithm, in comparison to the previous reaction-diffusion stereo algorithm and a state-of-the-art stereo algorithm.

In the future direction of the present research work, we are planning to dynamically integrate edge information into the reaction-diffusion stereo algorithm. That is, we first detect edge information from both distribution maps on image intensity and initially-detected disparity, which is obtained from an output of a matching cost function. Next, we compute tentative disparity distribution by integrating the firstly detected edge information into the reaction-diffusion stereo algorithm having anisotropic diffusion. By repeating the two steps of edge detection and stereo disparity detection alternately, we update stereo disparity distribution so as to achieve better performance of the reaction-diffusion stereo algorithm. The present position paper is the first step in this future direction.

2 REACTION-DIFFUSION

The FitzHugh-Nagumo type reaction-diffusion equations consist of two time-evolving partial differential equations with two variables: activator and inhibitor. The equations were proposed as a model of signal propagation along a nerve axon (FitzHugh, 1961; Nagumo et al., 1962). Let us consider two-dimensional space (x,y) and time t; let $u(x,y,t)$ be the activator variable and $v(x,y,t)$ be the inhibitor variable. Then, the reaction-diffusion equations are described as follows:

$$\partial_t u = D_u \nabla^2 u + [u(u-a)(1-u) - v]/\varepsilon, \quad (1)$$

$$\partial_t v = D_v \nabla^2 v + (u - bv), \quad (2)$$

where ∂_t denotes $\partial/\partial t$ and ∇ denotes the two-dimensional spatial gradient operator; D_u is a diffusion coefficient on the activator $u(x,y,t)$, D_v is a diffusion coefficient on the inhibitor $v(x,y,t)$, and ε is a positive small constant ($0 < \varepsilon \ll 1$).

The diffusion-less system derived from Eqs. (1) and (2) behaves as two different types of system: bi-stable system and mono-stable system, depending on the parameter values of a and b. The bi-stable system has two stable steady states and the mono-stable system has the one stable steady state; the stable steady states satisfy $u(u-a)(1-u) - v = 0$ and $u - bv = 0$.

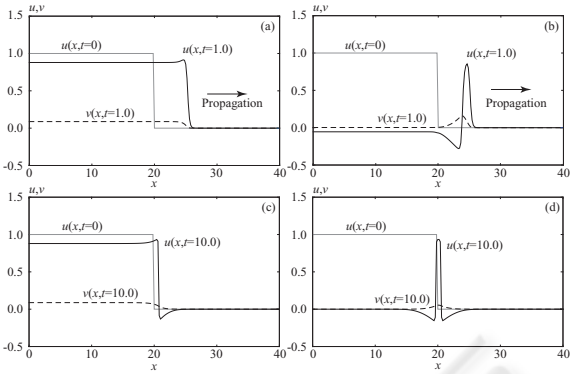

Figure 1: Numerical results on the reaction-diffusion Eqs. (1) and (2) in one-dimensional space x. The parameter values utilized here are as follows. (a) $D_v = 0.0$, $\varepsilon = 1.0 \times 10^{-2}$, $b = 10$; (b) $D_v = 0.0$, $\varepsilon = 1.0 \times 10^{-2}$, $b = 1.0$; (c) $D_v = 10.0$, $\varepsilon = 1.0 \times 10^{-3}$, $b = 10$; (d) $D_v = 10.0$, $\varepsilon = 1.0 \times 10^{-3}$, $b = 1.0$. We fixed the other parameter values of D_u and a at $D_u = 1.0$ and $a = 0.05$ and discretized space x with the finite difference $\delta x = 1/5$ and time t with the finite difference $\delta t = 1/1000$ for the numerical computation. The system of Eqs. (1) and (2) is bi-stable in (a) and (c), and mono-stable in (b) and (d). A solid black line indicates $u(x, t = 1.0)$ or $u(x, t = 10.0)$, and a broken line indicates $v(x, t = 1.0)$ or $v(x, t = 10.0)$ in each figure. A solid gray line indicates an initial condition for $u(x, t = 0)$ in each figure; an initial condition for $v(x, t = 0)$ was fixed at $v = 0$ over the entire space x. A wave front or a wave pulse propagates towards a right arrow in each of (a) and (b); a wave front or a wave pulse does not propagate but remains at the center edge position in the one dimensional space x in (c) and (d).

As time proceeds, any solution converges to either of the two stable steady states in the bi-stable system, and to the stable steady state in the mono-stable system.

The set of the reaction-diffusion Eqs. (1) and (2) generates a traveling wave under the condition $D_u > D_v$. Figure 1(a) shows a propagating wave front generated by the bi-stable system; Fig. 1(b) shows a propagating pulse wave generated by the mono-stable system. In the both cases, a wave front or a pulse wave propagates at almost constant velocity in one-dimensional space. The propagation velocity depends on the parameter values of D_u, a and ε.

When the set of Eqs. (1) and (2) is in the condition $D_u \ll D_v$, it generates a static pattern (Turing, 1952). Under the condition $D_u \ll D_v$, the inhibitor v diffuses more rapidly than the activator u. Since the increasing inhibitor variable v prevents the activator variable u from increasing, it prevents the wave front or the pulse wave from propagating. That is, we obtain a static pattern of the wave front or the pulse wave.

The authors found that the set of Eqs. (1) and (2) has two functions applicable to image processing (Nomura et al., 2003). They found that the bi-

stable system can detect segments and the monostable system can detect edges from image intensity distribution given to the initial condition of $u(x,y,t=0)$. The parameter a in Eq. (1) works as a threshold level for segmentation and edge detection. Figures 1(c) and 1(d) show one-dimensional examples of segmentation and edge detection on a step function given to the initial condition of $u(x,t=0)$.

In addition to segmentation and edge detection, the authors proposed a stereo algorithm that utilizes multi-sets of the FitzHugh-Nagumo type reaction-diffusion equations (Nomura et al., 2009). They connected the bi-stable systems of the reaction-diffusion equations through the parameter a as follows:

$$\begin{aligned}\partial_t u_d &= D_u\nabla^2 u_d + \mu C_d \\ &\quad +[u_d(1-u_d)(u_d - a_d(u_{\max})) - v_d]/\varepsilon, \quad (3)\\ \partial_t v_d &= D_v\nabla^2 v_d + (u_d - b v_d), \quad (4)\end{aligned}$$

where $u_d(x,y,t)$ and $v_d(x,y,t)$ are activator and inhibitor variables in each set of the reaction-diffusion equations, and μ is a constant that controls an external stimulus of a matching cost function $C_d(x,y)$ with a disparity level d. Thus, each of the sets governs areas associated with the disparity level d. A wave front associated with the disparity level d propagates into undefined disparity areas, according to the diffusion of the activator variable u; thus, the wave front propagation realizes the continuity constraint imposed on the stereo algorithm. A mutual inhibition mechanism built into the multi-sets of the equations through the next function $a_d(u_{\max})$ realizes the uniqueness constraint as follows:

$$\begin{aligned}a_d(u_{\max}) &= a_0 + \frac{u_{\max}}{2}[1+\tanh(d_a - a_1)],\\ u_{\max} &= \max_{d'\in\Theta} u_{d'},\\ d_a &= \left| d - \arg\max_{d'\in\Theta} u_{d'} \right| \quad (5)\end{aligned}$$

where a_0 and a_1 are constants and Θ denotes the inhibition area for the uniqueness constraint (Zitnick and Kanade, 2000).

The finite difference method with the spatial finite differences of δx and δy and the temporal finite difference of δt discretizes partial differential operators ∇ and $\partial/\partial t$. For example, the Gauss-Seidel method provides a solution to a set of linear equations derived from Eqs. (3) and (4). After enough duration of time t, the next equation provides a disparity map $M(x,y,t)$ as follows:

$$M(x,y,t) = \arg\max_{d\in\Delta} u_d(x,y,t), \quad (6)$$

where Δ denotes a set of possible disparity levels.

3 PROPOSED INTEGRATION ALGORITHM

Depth discontinuity causes numerous errors in the previous stereo algorithm utilizing multi-sets of the reaction-diffusion equations. As mentioned in the previous section, a propagating wave front fills in undefined disparity areas; this filling-in process realizes the continuity constraint. However, the filling-in process causes error around areas having the depth discontinuity. In order to reduce errors around the areas, we need to prevent the filling-in process, that is, to prevent the wave front from propagating across depth edges.

Areas having depth discontinuity are generally unknown prior to stereo disparity detection. Poggio et al. proposed a visual integration algorithm that detects depth discontinuity, by integrating intensity edge information and stereo disparity distribution (Poggio et al., 1988). Thus, instead of taking account of the areas having the depth discontinuity, we utilize edges detected for image intensity distribution in the stereo algorithm. The authors also proposed another reaction-diffusion algorithm designed for edge detection (Nomura et al., 2008). Thus, the two variables $u(x,y,T)$ and $v(x,y,T)$ obtained by the reaction-diffusion algorithm after finite duration of time T are useful as intensity edge information. Let $u_e(x,y)$ be $u(x,y,T)$ and $v_e(x,y)$ be $v(x,y,T)$; high values in $u_e(x,y)$ and $v_e(x,y)$ denote the existence of edges, as shown in Fig. 1(d).

Now, we modify the reaction-diffusion Eqs. (3) and (4) in order to integrate edge information into the stereo algorithm. Let us recall that a single set of the reaction-diffusion Eqs. (1) and (2) generates a wave front propagating at a velocity. The velocity depends on the diffusion coefficient D_u and decreases as D_u decreases, when other parameter values are fixed. Thus, we propose to introduce the intensity edge information denoted by u_e and v_e into the diffusion terms as follows:

$$\begin{aligned}\partial_t u_d &= D_u\nabla\cdot[(1-u_e)\nabla u_d] + \mu C_d \\ &\quad +[u_d(1-u_d)(u_d - a_d(u_{\max})) - v_d]/\varepsilon, \quad (7)\\ \partial_t v_d &= D_v\nabla\cdot[(1-v_e)\nabla v_d] + u_d - b v_d, \quad (8)\end{aligned}$$

where $\nabla\cdot[(1-u_e)\nabla u_d]$ and $\nabla\cdot[(1-v_e)\nabla v_d]$ describe the anisotropic diffusion fields. The two terms $(1-u_e)$ and $(1-v_e)$ weaken the diffusion of u_d and v_d around the edge areas.

Table 1: Quantitative performance evaluations on the four stereo image pairs: CONES, TEDDY, TSUKUBA and VENUS. We evaluated stereo disparity maps with the bad-match-percentage error measure having the threshold level of 1.0 (pixel) in non-occlusion area (nonocc.), all area (all) and area having depth-discontinuity (disc.). Stereo algorithms evaluated here are as follows: the reaction-diffusion algorithm (RD), the reaction-diffusion algorithm with the integration of intensity edge information (RD+IE), the state-of-the-art algorithm (AdaptingBP: ABP) (Klaus et al., 2006). We fixed the parameter values of the reaction-diffusion stereo algorithms across the four stereo image pairs. The Middlebury website (http://vision.middlebury.edu/stereo/) provides the stereo image pairs, the ground truth data and definitions of the areas as well as the scores on the state-of-the-art algorithm. See also Figs. 2 and 3 on the results of the reaction-diffusion algorithms.

		RD	RD+IE	ABP
CONES	nonocc.	5.53	5.36	2.48
	all	12.57	12.98	7.92
	disc.	15.18	14.45	7.32
TEDDY	nonocc.	14.85	14.68	4.22
	all	20.86	20.91	7.06
	disc.	30.15	29.06	11.8
TSUKUBA	nonocc.	5.98	8.46	1.11
	all	7.86	10.19	1.37
	disc.	19.70	20.13	5.79
VENUS	nonocc.	2.75	2.93	0.10
	all	3.92	4.09	0.21
	disc.	21.23	20.18	1.44

4 EXPERIMENTAL RESULTS

This section presents experimental results on the well-known four test stereo image pairs: CONES, TEDDY, TSUKUBA and VENUS, all of which are provided on the Middlebury website (http://vision.middlebury.edu/stereo/) with their ground truth data and definitions of areas having depth discontinuity. We applied two reaction-diffusion stereo algorithms to the four stereo image pairs; one of the two stereo algorithms is the previous algorithm proposed by the authors (Nomura et al., 2009) and the other one is the proposed algorithm integrating intensity edge information.

Figures 2 and 3 show results of stereo disparity detection on CONES and TEDDY. Let us focus on areas surrounded by red broken lines in Figs. 2 and 3. The proposed algorithm detected disparity values correctly along the areas having the depth discontinuity, in comparison to the results detected by the previous reaction-diffusion algorithm. In these areas, detected intensity edges coincide quite well with the edges having the depth discontinuity.

We quantitatively evaluated the stereo disparity maps with respect to the bad-match-percentage error measure. Table 1 shows the results of the evaluations. Although the performance of the proposed algorithm is rather better than the performance of the previous algorithm for the areas having the depth discontinuity (disc.) on the stereo image pairs: CONES, TEDDY and VENUS, it becomes worse for the all areas (all) and on the image pair TSUKUBA. Table 1 also shows the results evaluated for the top-ranked state-of-the-art algorithm (Klaus et al., 2006). We recognize that the quantitative performance of the reaction-diffusion algorithm is much worse than that of the state-of-the-art algorithm.

5 CONCLUSIONS

In the present paper, we have proposed a visual integration algorithm that integrates intensity edge information into a reaction-diffusion stereo algorithm (Nomura et al., 2009) for improving its performance around areas having depth discontinuity. We provide intensity edge information obtained by another reaction-diffusion algorithm designed for edge detection to anisotropic diffusion fields of multi-sets of the reaction-diffusion equations utilized in the stereo algorithm. Stereo disparity maps obtained for test stereo image pairs show that success of the proposed algorithm was observed in part around the areas having depth discontinuity. However, the quantitative performance evaluated for the proposed algorithm was not superior but almost similar to the previous reaction-diffusion stereo algorithm. There are several areas in which the proposed algorithm does not work, even if detected intensity edges coincide with depth edges. Thus, we need to observe the situation causing errors and to consider how to suppress the errors around areas having the depth discontinuity. This is the next work required to establish the proposed stereo algorithm.

ACKNOWLEDGEMENTS

The present study was supported in part by the Grant-in-Aid for Scientific Research (C) (No. 20500206) from the Japan Society for the Promotion of Science.

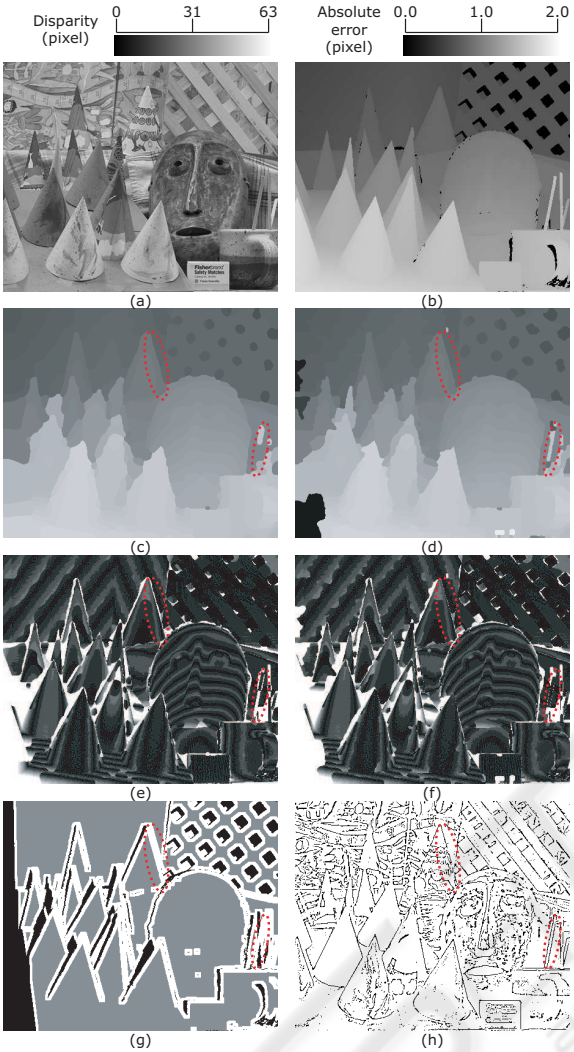

Figure 2: Experimental results on the stereo image pair CONES. (a) Left image of the pair and (b) ground truth disparity map. Image size is 450×375 (pixels^2) and possible disparity levels are $\Delta = \{0, 1, \cdots, 59\}$ (pixels). (c) Stereo disparity map $M(x, y, t = 100)$ detected by the previous reaction-diffusion stereo algorithm; (d) that detected by the proposed algorithm. (e) Absolute error map on the detected map (c); (f) that on (d). (g) Definition of area having depth discontinuity (white area) and non-occlusion area (gray area). (h) Edge detection result obtained for the left image (a) by the reaction-diffusion algorithm designed for edge detection (Nomura et al., 2008); black dots and lines indicate detected intensity edges. Parameter values of the two stereo algorithms were fixed as $\delta x = \delta y = 1/5$, $\delta t = 1/100$, $D_u = 1.0$, $D_v = 3.0$, $a_0 = 0.13$, $a_1 = 1.5$, $b = 10$, $\varepsilon = 1.0 \times 10^{-2}$ and $\mu = 3.0$. See the literature (Nomura et al., 2008) for parameter values utilized in (h). Table 1 shows results of the quantitative performance evaluations. The Middlebury website (http://vision.middlebury.edu/stereo/) provides the stereo image pair, the ground truth data and the definitions of the areas.

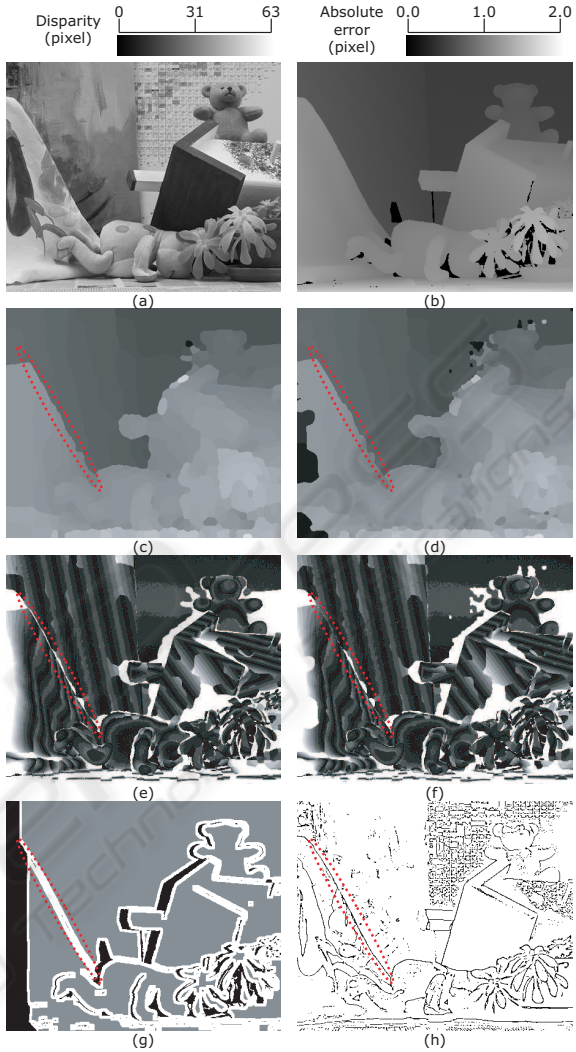

Figure 3: Experimental results on the stereo image pair TEDDY. (a) Left image of the pair and (b) ground truth disparity map. Image size is 450×375 (pixels^2) and possible disparity levels are $\Delta = \{0, 1, \cdots, 59\}$ (pixels). (c) Stereo disparity map $M(x, y, t = 100)$ detected by the previous reaction-diffusion stereo algorithm; (d) that detected by the proposed algorithm. (e) Absolute error map on the detected map (c); (f) that on (d). (g) Definition of area having depth discontinuity (white area) and non-occlusion area (gray area). (h) Edge detection result obtained for the left image (a) by the reaction-diffusion algorithm designed for edge detection (Nomura et al., 2008); black dots and lines indicate detected intensity edges. Parameter values of the two stereo algorithms were fixed as $\delta x = \delta y = 1/5$, $\delta t = 1/100$, $D_u = 1.0$, $D_v = 3.0$, $a_0 = 0.13$, $a_1 = 1.5$, $b = 10$, $\varepsilon = 1.0 \times 10^{-2}$ and $\mu = 3.0$. See the literature (Nomura et al., 2008) for parameter values utilized in (h). Table 1 shows results of the quantitative performance evaluations. The Middlebury website (http://vision.middlebury.edu/stereo/) provides the stereo image pair, the ground truth data and the definitions of the area.

REFERENCES

Adamatzky, A., Costello, B. D. L., and Asai, T. (2005). *Reaction-Diffusion Computers*. Elsevier, Amsterdam.

Black, M. J., Sapiro, G., Marimont, D. H., and Heeger, D. (1998). Robust anisotropic diffusion. *IEEE Transactions on Image Processing*, 7(3):421–432.

Deng, Y., Yang, Q., Lin, X., and Tang, X. (2007). Stereo correspondence with occlusion handling in a symmetric patch-based graph-cuts model. *IEEE Transactions on Pattern Analysis and Machine Intelligence*, 29(6):1068–1079.

FitzHugh, R. (1961). Impulses and physiological states in theoretical models of nerve membrane. *Biophysical Journal*, 1:445–466.

Klaus, A., Sormann, M., and Karner, K. (2006). Segment-based stereo matching using belief propagation and a self-adapting dissimilarity measure. In *Proceedings of the 18th International Conference on Pattern Recognition*, volume 3, pages 15–18, New York. IEEE Press.

Kuhnert, L. (1986). A new optical photochemical memory device in a light-sensitive chemical active medium. *Nature*, 319:393–394.

Kuhnert, L., Agladze, K. I., and Krinsky, V. I. (1989). Image processing using light-sensitive chemical waves. *Nature*, 337:244–247.

Landy, M. S., Maloney, L. T., Johnston, E. B., and Young, M. (1995). Measurement and modeling of depth cue combination: in defense of weak fusion. *Vision Research*, 35(3):389–412.

Marr, D. and Poggio, T. (1979). A computational theory of human stereo vision. *Proceedings of the Royal Society of London. Series B, Biological Sciences*, 204(1156):301–328.

Nagumo, J., Arimoto, S., and Yoshizawa, S. (1962). An active pulse transmission line simulating nerve axon. *Proceedings of the IRE*, 50(10):2061–2070.

Nomura, A., Ichikawa, M., and Miike, H. (2009). Reaction-diffusion algorithm for stereo disparity detection. *Machine Vision and Applications*. DOI:10.1007/s00138-007-0117-8 (in press).

Nomura, A., Ichikawa, M., Miike, H., Ebihara, M., Mahara, H., and Sakurai, T. (2003). Realizing visual functions with the reaction-diffusion mechanism. *Journal of the Physical Society of Japan*, 72(9):2385–2395.

Nomura, A., Ichikawa, M., Sianipar, R. H., and Miike, H. (2008). Edge detection with reaction-diffusion equations having a local average threshold. *Pattern Recognition and Image Analysis*, 18(2):289–299.

Perona, P. and Malik, J. (1990). Scale-space and edge detection using anisotropic diffusion. *IEEE Transactions on Pattern Analysis and Machine Intelligence*, 12(7):629–639.

Poggio, T., Gamble, E. B., and Little, J. J. (1988). Parallel integration of vision modules. *Science*, 242(4877):436–440.

Scharstein, D. and Szeliski, R. (2002). A taxonomy and evaluation of dense two-frame stereo correspondence algorithms. *International Journal of Computer Vision*, 47(1-3):7–42.

Suzuki, Y., Takayama, T., Motoike, I. N., and Asai, T. (2005). A reaction-diffusion model performing stripe- and spot-image restoration and its LSI implementation. *Transactions of IEICE*, J88-A(11):1272–1281. (in Japanese).

Turing, A. M. (1952). The chemical basis of morphogenesis. *Philosophical Transactions of the Royal Society of London. Series B, Biological Sciences*, 237(641):37–72.

Ueyama, E., Yuasa, H., Hosoe, S., and Ito, M. (1998). Figure-ground separation from motion with reaction-diffusion equation – the front of the generated pattern and a subjective contour –. *IEICE Transactions on Information and Systems*, J81-D-II(12):2767–2778. (in Japanese).

Zitnick, C. L. and Kanade, T. (2000). A cooperative algorithm for stereo matching and occlusion detection. *IEEE Transactions on Pattern Analysis and Machine Intelligence.*, 22(7):675–684.